Organometallics 1992, 11, 4001-4009

Cluster Synthesis. 40. New High-Nuclearity Platinum–Ruthenium Carbonyl Cluster Complexes. Synthesis and Structural Characterizations of $Ru_8Pt_2(CO)_{23}(\mu_3\text{-}H)_2$, $Ru_7Pt_3(CO)_{22}(\mu_3\text{-}H)_2$, and $Ru_8Pt_2(CO)_{21}(\mu_3\text{-}\eta^2\text{-}CO)_2(dppe)(\mu\text{-}H)_2$ with a New Type of Triply Bridging CO Ligand and the New Layered Cluster Complex $Ru_6Pt_3(CO)_{21}(\mu\text{-}CO)(\mu_3\text{-}H)_2$

Richard D. Adams,* Zhaoyang Li, Jau-Ching Lii, and Wengan Wu

Department of Chemistry and Biochemistry, University of South Carolina, Columbia, South Carolina 29208

Received June 15, 1992

The reaction of $Ru_4Pt_2(CO)_{18}$ with $Ru_4(CO)_{13}(\mu\text{-}H)_2$ at 97 °C yielded the new decanuclear platinum–ruthenium carbonyl cluster complex $Ru_8Pt_2(CO)_{23}(\mu_3\text{-}H)_2$, 1 (22%). In a similar manner the reaction of $Ru_4Pt_2(CO)_{18}$ with $Ru_3Pt(CO)_{10}(COD)(\mu\text{-}H)_2$ at 97 °C yielded the new decanuclear platinum–ruthenium carbonyl cluster complex $Ru_7Pt_3(CO)_{21}(\mu\text{-}CO)(\mu_3\text{-}H)_2$, 2, in 25% yield. Both compounds were characterized by IR, ^1H NMR, and single-crystal X-ray diffraction analyses, and both were found to consist of similar edge-fused bioctahedral clusters with platinum atoms along the edge-sharing sites. There are strong metal–metal bonds between the apices of the adjacent octahedra. Both compounds are electron deficient, and one of the apical–apical Ru–Ru bonds is unusually short, 2.580 (2) Å in 1 and 2.593 (5) Å in 2. The hydrides are triply bridging ligands, and these were located and refined crystallographically in 1. The reaction of 1 with 1,2-bis(diphenylphosphino)ethane, dppe, yielded the adduct $Ru_8Pt_2(CO)_{21}(\mu_3\text{-}CO)_2(dppe)(\mu\text{-}H)_2$, 3, in 12% yield, which was shown to consist of a face-shared bioctahedral cluster of seven ruthenium and two platinum atoms with a ruthenium "spike" containing the dppe ligand extending from one triruthenium face. Two novel dihapto–triply bridging carbonyl ligands were found to bridge to the ruthenium spike. 1 and 2 both react with CO at 25 °C, but only the product obtained from the reaction of 2, $Ru_6Pt_3(CO)_{21}(\mu\text{-}CO)(\mu_3\text{-}H)_2$, 4 (55% yield), could be fully characterized. It was shown to contain a cluster of nine metal atoms arranged into trinuclear layers of pure ruthenium and pure platinum. The two triply bridging hydride ligands were located and refined crystallographically. Crystal data: for 1, space group $P2_1/n$, a = 20.454 (3) Å, b = 17.676 (4) Å, c = 10.219 (2) Å, β = 90.42 (1)°, 2584 reflections, and R = 0.031; for 2, space group $P2_1/n$, a = 9.838 (3) Å, b = 20.262 (4) Å, c = 18.299 (3) Å, β = 91.47 (2)°, 2104 reflections, and R = 0.045; for $3\cdot{}^3/_4\ CH_2Cl_2$, space group $P2_1/c$, a = 10.503 (2) Å, b = 20.659 (4) Å, c = 28.379 (5) Å, β = 94.36 (1)°, 4553 reflections, and R = 0.032; for 4, space group $P2_1/c$, a = 21.314 (4) Å, b = 16.544 (4) Å, c = 22.318 (4) Å, β = 116.89 (1)°, 4509 reflections, and R = 0.031.

Introduction

Due to the importance of bimetallic platinum alloys to the process of catalytic petroleum reforming,[1] there has developed a great interest in the chemistry of heteronuclear cluster complexes containing platinum.[2] Higher nuclearity mixed-metal clusters might serve as models for such heterogeneous catalysts and could produce similar transformations of organic molecules on their surfaces.

It has been shown that $Pt(COD)_2$, COD = 1,5-cyclooctadiene, can be a valuable reagent for the synthesis of heteronuclear cluster complexes containing platinum.[1,3-9] Our recent research has been focused on the study of high-nuclearity cluster complexes of platinum combined with metals of the iron subgroup.[4-10] We have recently prepared the new cluster complex $Ru_4Pt_2(CO)_{18}$ from the reaction of $Pt(COD)_2$ with ruthenium pentacarbonyl.[5]

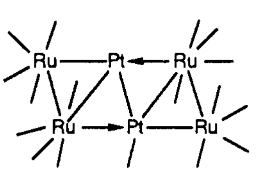

$Ru_4Pt_2(CO)_{18}$

We have now found that this complex readily combines with the hydride-containing tetranuclear metal carbonyl complexes $Ru_4(CO)_{13}(\mu\text{-}H)_2$ and $Ru_3Pt(CO)_{10}(COD)(\mu\text{-}H)_2$ to yield the new decanuclear platinum–ruthenium carbonyl complexes $Ru_8Pt_2(CO)_{23}(\mu_3\text{-}H)_2$, 1, and $Ru_7Pt_3(CO)_{22}(\mu_3\text{-}H)_2$, 2, respectively, containing hydride ligands. The synthesis and characterization of these complexes is described in this report together with the results of a study of their reactions with the simple donor ligands CO and 1,2-bis(diphenylphosphino)ethane, dppe. A preliminary

---

[1] (a) Sinfelt, J. H. *Bimetallic Catalysts. Discoveries, Concepts and Applications*; Wiley: New York, 1983. (b) Sinfelt, J. H. *Sci. Am.* **1985**, *253*, 90. (c) Sinfelt, J. H. *Acc. Chem. Res.* **1977**, *10*, 15. (d) Sachtler, W. M. H. *J. Mol. Catal.* **1984**, *25*, 1. (e) Ponec, V. *Adv. Catal.* **1983**, *32*, 149. (f) Biswas, J.; Bickle, G. M.; Gray, P. G.; Do, D. D.; Barbier, J. *Catal. Rev.—Sci. Eng.* **1988**, *30*, 161.

[2] (a) Farrugia, L. J. *Adv. Organomet. Chem.* **1990**, *31*, 301. (b) Braunstein, P.; Rose, J. In *Stereochemistry of Organometallic and Inorganic Compounds*; Bernal, I., Ed.; Elsevier: Amsterdam, 1989; Vol. 3.

[3] (a) Couture, C.; Farrar, D. H.; Goudsmit, R. J. *Inorg. Chim. Acta* **1984**, *89*, L29. (b) Couture, C.; Farrar, D. H. *J. Chem. Soc., Chem. Commun.* **1985**, 197. (c) Couture, C.; Farrar, D. H. *J. Chem. Soc., Dalton Trans.* **1986**, 1395. (d) Couture, C.; Farrar, D. H. *J. Chem. Soc., Dalton Trans.* **1987**, 2245. (e) Couture, C.; Farrar, D. H. *J. Chem. Soc., Dalton Trans.* **1987**, 2253.

[4] Adams, R. D.; Arafa, I.; Chen, G.; Lii, J. C.; Wang, J. G. *Organometallics* **1990**, *9*, 2350.

[5] Adams, R. D.; Chen, G.; Wang, J. G.; Wu, W. *Organometallics* **1990**, *9*, 1339.

[6] Adams, R. D.; Chen, G.; Lii, J. C.; Wu, W. *Inorg. Chem.* **1991**, *30*, 1007.

[7] Adams, R. D.; Lii, J. C.; Wu, W. *Inorg. Chem.* **1991**, *30*, 3613.

[8] Adams, R. D.; Alexander, M. S.; Arafa, I.; Wu, W. *Inorg. Chem.* **1991**, *30*, 4717.

[9] Adams, R. D.; Li, Z.; Lii, J. C.; Wu, W. *Inorg. Chem.* **1992**, *31*, 3445.

[10] (a) Adams, R. D.; Lii, J. C.; Wu, W. *Inorg. Chem.* **1992**, *31*, 2556. (b) Adams, R. D.; Lii, J. C.; Wu, W. *Inorg. Chem.* **1991**, *30*, 2257.

0276-7333/92/2311-4001$03.00/0

report on a portion of these studies has been published.[11]

Experimental Section

General Procedures. All the reactions were performed under an atmosphere of nitrogen unless otherwise indicated. Reagent grade solvents were dried over sodium and deoxygenated by purging with N_2 prior to use. $Ru_4(CO)_{13}(\mu\text{-H})_2$,[12] $Ru_3Pt(CO)_{10}(COD)(\mu\text{-H})_2$,[9] and $Ru_4Pt_2(CO)_{18}$[5] were prepared according to the literature. 1,2-Bis(diphenylphosphino)ethane, dppe, was purchased from Aldrich and was used without further purification. IR spectra were recorded on a Nicolet 5DXB FT-IR spectrophotometer. ^1H NMR spectra were recorded on a Bruker AM-300 FT-NMR spectrometer. Elemental microanalyses were performed by Desert Analytics, Tucson, AZ, and Oneida Research Services Inc., Whitesboro, NY. TLC separations were performed in air by using silica gel (60 Å, F_{254}) on plates (Whatman, 0.25 mm).

Synthesis of $Ru_8Pt_2(CO)_{23}(\mu\text{-H})_2$, 1. A 30.0-mg amount of $Ru_4Pt_2(CO)_{18}$ (0.0231 mmol) and 18.0-mg amount of $Ru_4(CO)_{13}(\mu\text{-H})_2$ (0.0233 mmol) were combined and dissolved in 40 mL of heptane at 25 °C. The resultant solution was heated to a gentle reflux and maintained for 43 min. After the solution was cooled to room temperature, the solvent was removed. The residue was then separated by TLC on silica gel by using a hexane/CH_2Cl_2 (3/1) solvent mixture. This yielded in order of elution 2.1 mg of a yellow mixture of $Ru_4(CO)_{12}(\mu\text{-H})_4$ and $Ru_3(CO)_{12}$, 12.0 mg of unreacted $Ru_4(CO)_{13}(\mu\text{-H})_2$, 2.1 mg of unreacted $Ru_4Pt_2(CO)_{18}$, and 8.9 mg of dark green $Ru_8Pt_2(CO)_{23}(\mu_3\text{-H})_2$, **1** (22% yield). Data for **1** follows. IR (ν(CO) in CH_2Cl_2): 2073 (vs), 2046 (m), 2033 (m), 2006 (w), 1975 (w) cm^{-1}. ^1H NMR (δ in CD_2Cl_2): −15.79 (s, 2 H, $^2J_{Pt-H}$ = 22.2 Hz). Anal. Calc (found): C, 14.97 (14.69); H, 0.11 (0.22).

Synthesis of $Ru_7Pt_3(CO)_{22}(\mu_3\text{-H})_2$, 2. A 50.0-mg amount of $Ru_4Pt_2(CO)_{18}$ (0.0385 mmol) and 34.0 mg of $Ru_3Pt(CO)_{10}(COD)(\mu\text{-H})_2$ (0.0383 mmol) were dissolved in 50 mL of heptane. The resultant solution was heated to a gentle reflux and maintained for 25 min. After cooling, the solvent was removed, and the residue was separated by TLC on silica gel with a hexane/CH_2Cl_2 (3/1) solvent mixture. This yielded in order of elution a yellow band containing 2.5 mg of a mixture of $Ru_4(CO)_{12}(\mu\text{-H})_4$ and $Ru_3(CO)_{12}$, 18.0 mg of yellow-green $Ru_7Pt_3(CO)_{22}(\mu_3\text{-H})_2$, **2** (25% yield), and 3.0 mg of orange $Ru_4Pt(CO)_{12}(\mu_4\text{-}\eta^2\text{-CO})(COD)$ (7%).[8] Data for **2** are as follows. IR (ν(CO) in CH_2Cl_2): 2068 (vs), 2046 (m), 2033 (m), 2020 (sh), 2005 (vw), 1964 (vw) cm^{-1}. ^1H NMR (δ in CD_2Cl_2): −9.83 (d, 1 H, J_{Pt-H} = 24.7 Hz, J_{H-H} = 1.0 Hz), −19.56 (d, 1H, J_{Pt-H} = 19.2 Hz, J_{H-H} = 1.0 Hz). Anal. Calc (found): C, 13.83 (13.84); H, 0.11 (0.23).

Reaction of 1 with dppe. A 22.0-mg amount of **1** (0.0119 mmol) was dissolved in 40 mL of CH_2Cl_2. The solution was cooled to 0 °C, and a solution containing 8.5 mg of dppe (0.0214 mmol) in 5 mL of CH_2Cl_2 was added dropwise. After 45 min at 0 °C, the solvent was removed in vacuo, and the residue was separated by TLC on silica gel by using a 5/3 CH_2Cl_2/hexane solvent mixture. This yielded in order of elution 1.0 mg of a dark-brown unidentified compound and 3.3 mg of blue-green $Ru_8Pt_2(CO)_{23}(\mu\text{-H})_2(dppe)$, **3** (12%). Data for **3** are as follows. IR (ν(CO) in CH_2Cl_2): 2084 (m), 2053 (s), 2039 (s, sh), 2030 (vs), 1963 (w), 1606 (m) cm^{-1}. ^1H NMR (δ in CD_2Cl_2 −57 °C): −7.70 (dd, 1H, J_{P-H}(cis) = 10 Hz, J_{P-H}(trans) = 29 Hz), −18.09 (s, 1 H). Anal. Calc (found): C, 25.93 (25.69); H, 1.20 (1.21).

Synthesis of 3 Enriched with ^{13}CO. $Ru_3(CO)_{12}$ was enriched with ^{13}CO at 125 °C by using 99% ^{13}CO in a sealed Parr high-pressure reactor in ethanol solvent. This was converted to $Ru(CO)_5$ and $Ru_4(CO)_{13}(\mu\text{-H})_2$ using ^{13}CO. The $Ru(CO)_5$ was converted to $Pt_2Ru_4(CO)_{18}$ and was then allowed to react with the enriched $Ru_4(CO)_{13}(\mu\text{-H})_2$ to yield **1**. This was subsequently converted to **3** by reaction with dppe. Measurements by IR spectroscopy indicated that the CO ligands contained ^{13}CO in approximately 50% of the total amount. The IR spectrum of this sample showed a new absorption at 1568 cm^{-1} at approximately the same intensity of an absorption an 1606 cm^{-1}, which is attributed to the corresponding ^{12}CO absorption of the $\mu_3\text{-}\eta^2$-CO ligand.

Reaction of 2 with CO. An 18.0-mg amount of **2** (0.00942 mmol) was dissolved in 70 mL of CH_2Cl_2. The resultant solution was slowly purged with CO at room temperature for 3 h. The solvent was removed, and the residue was separated by TLC using a 2/1 hexane/CH_2Cl_2 solvent mixture. This yielded in order of elution 1.2 mg of a yellow mixture of $Ru_4(CO)_{12}(\mu\text{-H})_4$ and $Ru_3(CO)_{12}$, 0.9 mg of purple $Ru_4Pt_2(CO)_{18}$, a trace amount of yellow-green unreacted **2**, and 9.4 mg of brown-red $Ru_6Pt_3(CO)_{22}(\mu_3\text{-H})_2$, **4** (55%). Data for **4** are as follows. IR (ν(CO) in CH_2Cl_2): 2106 (vw), 2071 (s, sh), 2062 (vs), 2049 (s), 2031 (m), 1854 (vw) cm^{-1}. ^1H NMR (δ in $CDCl_3$): −17.19 (s, 2 H J_{Pt-H} = 17.0 Hz). Anal. Calc (found): C, 14.60 (14.94), H, 0.11 (0.08).

Reaction of 1 with CO. A 5.0-mg amount of **1** (0.00271 mmol) was dissolved in 40 mL of CH_2Cl_2, and the solution was purged slowly with CO for 6 h. An IR spectrum of the solution showed the complete conversion of compound **1** to a unknown new compound. The solvent was removed. The ^1H NMR spectrum in $CDCl_3$ solvent showed two signals at −13.59 and −17.34 ppm. Efforts to obtain crystals yielded only black powders. IR spectra of the powder showed the same pattern as that of the reaction mixture. IR (ν(CO) in CH_2Cl_2): 2122 (m), 2091 (s), 2072 (vs), 2055 (m), 2028 (m), 2018 (sh), 2010 (sh) cm^{-1}. Efforts to obtain crystals suitable for X-ray diffraction analysis were not successful. The reaction of **1** (approximately 2.5 mg) with CO in $CDCl_3$ solvent in an NMR tube at 25 °C was followed by ^1H NMR spectroscopy for 4 days. The signal of **1** at −15.86 ppm was dominant after 1 h, but after 13 h the signal had disappeared and was replaced by the two signals at −13.59 and −17.34 ppm. These two signals remained unchanged after 4 days in solution.

Crystallographic Analyses. Crystals of compound **1** suitable for diffraction analyses were grown by slow evaporation of solvent from a solution of CH_2Cl_2/hexane (4/1) at 25 °C. Crystals of compound **2** were obtained by crystallization from a solution in CH_2Cl_2/hexane (1/4) at 25 °C. Crystals of compound **3** were grown in a solution of CH_2Cl_2/hexane (2/1) solvent mixture at 5 °C. Crystals of compound **4** were grown in a solution of CH_2Cl_2/cyclohexane (1/4) solvent mixture at 25 °C. All data crystals were mounted in thin-walled glass capillaries. Diffraction measurements were made on a Rigaku AFC6S fully automated four-circle diffractometer using graphite-monochromated Mo Kα radiation. The unit cells were determined and refined from 15 randomly selected reflections obtained by using the AFC6S automatic search, center, index, and least-squares routines. Intensity data were collected by using the ω-scan technique (moving crystal–stationary counter). All data processing was performed on a Digital Equipment Corp. VAXstation 3520 computer by using the TEXSAN structure solving program library (version 5.0) obtained from Molecular Structure Corp., The Woodlands, TX. Neutral-atom scattering factors were calculated by the standard procedures.[13a] Anomalous dispersion corrections were applied to all non-hydrogen atoms.[13b] Lorentz/polarization (Lp) and absorption corrections (empirical based on azimuthal scans of three reflections) were applied to the data for each structure. Full-matrix least-squares refinements minimized the function

$$\sum_{hkl} w(|F_o| - |F_c|)^2$$

where $w = 1/\sigma(F_o)^2$, $\sigma(F_o) = \sigma(F_o^2)/2F_o$, and $\sigma(F_o^2) = [\sigma(I_{raw})^2 + (0.02I_{net})^2]^{1/2}/Lp$.

All four compounds crystallized in the monoclinic crystal system. The space groups $P2_1/n$ for compounds **1** and **2** and $P2_1/c$ for compounds **3** and **4**, respectively, were identified uniquely on the basis of the systematic absences observed during the collection of data. Each structure was solved by a combination of direct methods (MITHRIL) and difference Fourier synthesis. For compounds **1** and **2** all the atoms heavier than carbon were refined with anisotropic thermal parameters and all carbon atoms were refined isotropically. The hydride ligands in **1** were located in difference Fourier maps and were successfully refined with iso-

---

[11] Adams, R. D.; Li, Z.; Lii, J.-C.; Wu, W. *J. Am. Chem. Soc.* **1992**, *114*, 4918.

[12] (a) Cauty, A. J.; Johnson, B. F. G.; Lewis, J. *J. Organomet. Chem.* **1972**, *43*, C35. (b) Cauty, A. J.; Johnson, B. F. G.; Lewis, J.; Norton, J. B. *J. Chem. Soc., Chem. Commun.* **1972**, 1331.

[13] *International Tables for X-ray Crystallography*; Kynoch Press: Birmingham, England, 1975; Vol. IV: (a) Table 2.2B, pp 99–101; (b) Table 2.3.1, pp 149–150.

Table I. Crystallographic Data for Diffraction Studies

	compd			
	1	2	3	4
empirical formula	$Pt_2Ru_8O_{23}C_{23}H_2$	$Pt_3Ru_7O_{22}C_{22}H_2$	$Pt_2Ru_8P_2O_{23}C_{49}H_{26}\cdot 0.75CH_2Cl_2$	$Pt_3Ru_6O_{22}C_{22}H_2$
fw	1844.99	1911.00	2270.72	1809.93
cryst system	monoclinic	monoclinic	monoclinic	monoclinic
lattice params				
a (Å)	20.454 (3)	9.838 (3)	10.503 (2)	21.314 (4)
b (Å)	17.676 (4)	20.262 (4)	20.659 (4)	16.544 (4)
c (Å)	10.219 (2)	18.299 (3)	28.379 (5)	22.318 (4)
β (deg)	90.42 (1)	91.47 (2)	94.36 (1)	116.89 (1)
V (Å^3)	3695 (2)	3647 (2)	6140 (2)	7019 (3)
space group	$P2_1/n$ (No. 14)	$P2_1/n$ (No. 14)	$P2_1/n$ (No. 14)	$P2_1/n$ (No. 14)
Z	4	4	4	8
D_{calc} (g/cm^3)	3.32	3.48	2.50	3.43
μ(Mo Kα) (cm^{-1})	108.2	144.2	66.5	145.8
abs corr	empirical	empirical	empirical	empirical
temp (°C)	20	20	20	20
$2\theta_{max}$ (deg)	42.0	40.0	40.0	40.0
no. of obs ($I > 3\sigma(I)$)	2584	2104	4553	4509
no. of variables	398	377	785	747
resids: R; R_w	0.031; 0.031	0.045; 0.043	0.032; 0.035	0.031, 0.030
goodness of fit	1.23	1.73	1.70	1.17
max shift in final cycle	0.05	0.02	0.19	0.24
largest peak in final diff map (e/Å^3)	0.86	1.53	1.30	1.00

tropic thermal parameters. For compound 2 the platinum atom Pt(3) was found to be disordered in a 50/50 amount with the ruthenium atom Ru(7). Refinement converged with 50% occupancy of each atom type at each of the two sites. The hydride ligands on 2 could not be located and were ignored.

For compound 3 all non-hydrogen atoms were refined anisotropically. The hydride ligands were located and were satisfactorily refined using fixed thermal parameters, $B = 4.0$. The positions of all hydrogen atoms on the phenyl rings were calculated by using idealized geometries. Their contributions were added to the structure factor calculations, but their positions were not refined. Nonintegral quantities, 0.50 and 0.25, of CH_2Cl_2 from the crystallization solvent were found cocrystallized with the complex about two different symmetry sites in the final stages of the analysis. This was included in the analysis and satisfactorily refined.

Compound 4 crystallized with two independent molecules in the asymmetric unit. Due to the size of the structure only the atoms heavier than carbon were refined with anisotropic thermal parameters. All carbon atoms were refined with isotropic thermal parameters. The positions of the hydride ligands were located and successfully refined with fixed thermal parameters. Crystallographic data are given in Table I.

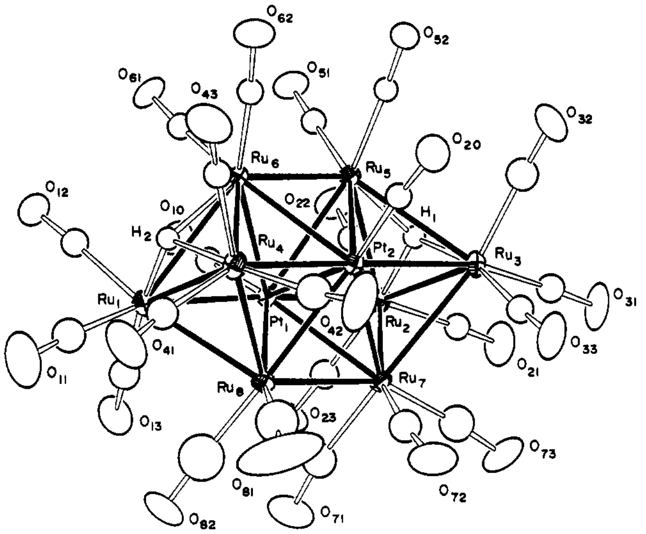

Figure 1. ORTEP drawing of $Ru_8Pt_2(CO)_{23}(\mu_3\text{-}H)_2$, 1, showing 50% probability thermal ellipsoids.

Results

The reactions of tetranuclear metal cluster dihydride complexes $Ru_4(CO)_{13}(\mu\text{-}H)_2$ and $Ru_3Pt(CO)_9(\mu\text{-}CO)(COD)(\mu\text{-}H)_2$ with $Ru_4Pt_2(CO)_{18}$ at 97 °C have yielded the two new decanuclear platinum-ruthenium carbonyl cluster complexes $Ru_8Pt_2(CO)_{23}(\mu_3\text{-}H)_2$, 1 (22%), and $Ru_7Pt_3(CO)_{22}(\mu_3\text{-}H)_2$, 2 (25%), respectively. Both compounds were characterized by IR, ^1H NMR, and single-crystal X-ray diffraction analyses.

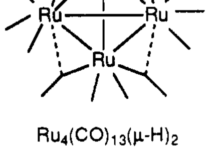

$Ru_4(CO)_{13}(\mu\text{-}H)_2$

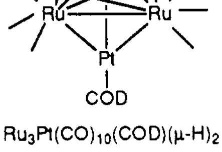

$Ru_3Pt(CO)_{10}(COD)(\mu\text{-}H)_2$

An ORTEP diagram of the structure of 1 is shown in Figure 1. Final atom positional parameters are listed in Table II. Selected interatomic distances and angles are listed in Tables III and IV. The molecule consists of a cluster of two edge-fused bioctahedra having the platinum atoms at the edge-shared sites. The Pt–Pt bond distance, 2.754 (1) Å, is slightly longer than platinum–platinum distances observed for triplatinum groupings in high-nuclearity platinum clusters.[7,9,10,14] There are strong metal–metal bonds between the apices of the fused octahedra, Ru(5)–Ru(6) = 2.580 (2) Å and Ru(7)–Ru(8) = 2.738 (2) Å. The Ru(5)–Ru(6) distance is much shorter than all of the other Ru–Ru distances in the molecule and may reflect the presence of the electron unsaturation; see below. The dianion $[Ru_{10}(CO)_{20}(\mu\text{-}CO)_4(\mu_6\text{-}C)_2]^{2-}$ has a similar fused bioctahedral structure[15] in which the apical–apical Ru–Ru bonds are very weak or perhaps nonexistent,[16] and in this ion the apical–apical Ru–Ru distances are much longer, 3.138 (2) and 3.122 (2) Å. Compound 1 contains two hydride ligands that were located and refined crystallographically which occupy triply bridging sites on the tri-

---

[14] (a) Longoni, G.; Chini, P. *J. Am. Chem. Soc.* **1976**, *98*, 7225. (b) Calabrese, J. C.; Dahl, L. F.; Chini, P.; Longoni, G.; Martinengo, S. *J. Am. Chem. Soc.* **1974**, *96*, 2614.

[15] Hayward, C.-M. T.; Shapley, J. R.; Churchill, M. R.; Bueno, C.; Rheingold, A. L. *J. Am. Chem. Soc.* **1982**, *104*, 7347.

[16] Ma, L.; Rodgers, D. P. S.; Wilson, S. R.; Shapley, J. R. *Inorg. Chem.* **1991**, *30*, 3591.

Table II. Positional Parameters and *B*(eq) Values (Å^2) for $Pt_2Ru_8(CO)_{23}(\mu_3\text{-}H)_2$, 1

atom	*x*	*y*	*z*	*B*(eq)
Pt(1)	0.19084 (04)	0.14990 (04)	0.47102 (07)	2.23 (4)
Pt(2)	0.20886 (04)	0.30018 (04)	0.53236 (07)	2.24 (3)
Ru(1)	0.05552 (08)	0.16272 (09)	0.46670 (16)	3.09 (8)
Ru(2)	0.32351 (08)	0.11817 (08)	0.48231 (15)	2.68 (8)
Ru(3)	0.34492 (08)	0.28099 (08)	0.54699 (16)	2.73 (8)
Ru(4)	0.07352 (08)	0.32881 (09)	0.53116 (16)	3.14 (8)
Ru(5)	0.26660 (07)	0.23960 (08)	0.31850 (14)	2.33 (7)
Ru(6)	0.14160 (07)	0.25895 (08)	0.31178 (14)	2.35 (7)
Ru(7)	0.25887 (08)	0.18978 (08)	0.68866 (14)	2.45 (7)
Ru(8)	0.12668 (08)	0.21351 (09)	0.67847 (15)	2.95 (8)
O(10)	0.1766 (07)	0.0351 (07)	0.2545 (13)	5.3 (8)
O(11)	−0.0852 (10)	0.1729 (12)	0.555 (02)	11 (2)
O(12)	0.0096 (09)	0.0950 (08)	0.2123 (15)	6 (1)
O(13)	0.0750 (09)	0.0025 (08)	0.5659 (18)	8 (1)
O(20)	0.2355 (08)	0.4616 (08)	0.4548 (16)	7 (1)
O(21)	0.4616 (08)	0.0709 (08)	0.5631 (18)	7 (1)
O(22)	0.3505 (08)	0.0414 (07)	0.2243 (14)	5.7 (9)
O(23)	0.2703 (07)	−0.0274 (07)	0.5900 (14)	5.4 (9)
O(31)	0.4826 (07)	0.2364 (09)	0.6258 (18)	7 (1)
O(32)	0.3976 (10)	0.4088 (10)	0.3808 (20)	9 (1)
O(33)	0.3378 (08)	0.3884 (09)	0.7758 (16)	7 (1)
O(41)	−0.0587 (09)	0.3313 (10)	0.6581 (19)	9 (1)
O(42)	0.1200 (09)	0.4524 (11)	0.713 (02)	10 (1)
O(43)	0.0263 (09)	0.4526 (08)	0.3486 (18)	8 (1)
O(51)	0.2812 (08)	0.1568 (07)	0.0648 (13)	5.0 (8)
O(52)	0.2913 (07)	0.3807 (07)	0.1619 (13)	4.7 (8)
O(61)	0.1227 (07)	0.1742 (08)	0.0653 (12)	4.9 (8)
O(62)	0.1310 (08)	0.3947 (07)	0.1401 (14)	6 (1)
O(71)	0.1977 (12)	0.0538 (10)	0.8272 (18)	11 (1)
O(72)	0.2291 (10)	0.2957 (08)	0.9179 (15)	8 (1)
O(73)	0.3832 (09)	0.1498 (13)	0.8321 (16)	9 (1)
O(81)	0.0701 (17)	0.3112 (17)	0.882 (02)	19 (3)
O(82)	0.0447 (18)	0.103 (02)	0.822 (02)	24 (3)
C(10)	0.1811 (10)	0.0764 (10)	0.3361 (19)	3.4 (4)
C(11)	−0.0317 (14)	0.1709 (13)	0.517 (02)	5.8 (6)
C(12)	0.0266 (11)	0.1226 (11)	0.306 (02)	3.9 (4)
C(13)	0.0653 (11)	0.0653 (12)	0.531 (02)	4.9 (5)
C(20)	0.2226 (10)	0.3979 (11)	0.4835 (18)	3.4 (4)
C(21)	0.4108 (11)	0.0913 (10)	0.5334 (19)	3.5 (4)
C(22)	0.3395 (10)	0.0729 (11)	0.321 (02)	3.9 (4)
C(23)	0.2894 (11)	0.0300 (12)	0.554 (02)	4.3 (5)
C(31)	0.4313 (12)	0.2521 (11)	0.590 (02)	4.2 (5)
C(32)	0.3793 (12)	0.3582 (13)	0.438 (02)	5.5 (5)
C(33)	0.3383 (10)	0.3468 (11)	0.6894 (20)	3.8 (4)
C(41)	−0.0118 (13)	0.3274 (12)	0.605 (02)	5.0 (5)
C(42)	0.1042 (14)	0.4031 (14)	0.651 (03)	6.3 (6)
C(43)	0.0448 (11)	0.4042 (11)	0.4093 (20)	3.8 (4)
C(51)	0.2762 (10)	0.1872 (10)	0.1645 (19)	3.2 (4)
C(52)	0.2839 (09)	0.3277 (10)	0.2224 (18)	2.9 (4)
C(61)	0.1278 (10)	0.2050 (10)	0.1612 (20)	3.4 (4)
C(62)	0.1356 (10)	0.3441 (10)	0.2131 (19)	3.4 (4)
C(71)	0.2157 (13)	0.1062 (14)	0.770 (02)	6.1 (6)
C(72)	0.2313 (12)	0.2595 (13)	0.826 (02)	5.3 (5)
C(73)	0.3372 (15)	0.1647 (14)	0.771 (03)	6.8 (6)
C(81)	0.0960 (17)	0.2741 (18)	0.798 (03)	9.5 (9)
C(82)	0.0762 (20)	0.1458 (19)	0.762 (04)	11 (1)
H(1)	0.330 (08)	0.210 (08)	0.430 (15)	4 (4)
H(2)	0.059 (08)	0.245 (08)	0.408 (15)	3 (4)

Table III. Intramolecular Distances for 1[a]

Pt(1)–Pt(2)	2.754 (1)	Ru(2)–H(1)	1.7 (1)
Pt(1)–Ru(1)	2.777 (2)	Ru(3)–Ru(5)	2.915 (2)
Pt(1)–Ru(2)	2.773 (2)	Ru(3)–Ru(7)	2.798 (2)
Pt(1)–Ru(5)	2.717 (2)	Ru(3)–C(31)	1.89 (2)
Pt(1)–Ru(6)	2.712 (2)	Ru(3)–C(32)	1.90 (2)
Pt(1)–Ru(7)	2.708 (2)	Ru(3)–C(33)	1.87 (2)
Pt(1)–Ru(8)	2.743 (2)	Ru(3)–H(1)	1.8 (1)
Pt(1)–C(10)	1.90 (2)	Ru(4)–Ru(6)	2.922 (2)
Pt(2)–Ru(3)	2.807 (2)	Ru(4)–Ru(8)	2.753 (2)
Pt(2)–Ru(4)	2.814 (2)	Ru(4)–C(41)	1.91 (3)
Pt(2)–Ru(5)	2.712 (2)	Ru(4)–C(42)	1.90 (3)
Pt(2)–Ru(6)	2.731 (2)	Ru(4)–C(43)	1.91 (2)
Pt(2)–Ru(7)	2.717 (2)	Ru(4)–H(2)	2.0 (1)
Pt(2)–Ru(8)	2.727 (2)	Ru(5)–Ru(6)	2.580 (2)
Pt(2)–C(20)	1.82 (2)	Ru(5)–C(51)	1.84 (2)
Ru(1)–Ru(4)	3.031 (2)	Ru(5)–C(52)	1.88 (2)
Ru(1)–Ru(6)	2.922 (2)	Ru(5)–H(1)	1.8 (2)
Ru(1)–Ru(8)	2.750 (2)	Ru(6)–C(61)	1.83 (2)
Ru(1)–C(11)	1.87 (3)	Ru(6)–C(62)	1.82 (2)
Ru(1)–C(12)	1.88 (2)	Ru(6)–H(2)	2.0 (2)
Ru(1)–C(13)	1.85 (2)	Ru(7)–Ru(8)	2.738 (2)
Ru(1)–H(2)	1.6 (1)	Ru(7)–C(71)	1.91 (3)
Ru(2)–Ru(3)	2.985 (2)	Ru(7)–C(72)	1.95 (2)
Ru(2)–Ru(5)	2.956 (2)	Ru(7)–C(73)	1.86 (3)
Ru(2)–Ru(7)	2.800 (2)	Ru(8)–C(81)	1.74 (3)
Ru(2)–C(21)	1.92 (2)	Ru(8)–C(82)	1.80 (4)
Ru(2)–C(22)	1.87 (2)	O–C(av)	1.15 (2)
Ru(2)–C(23)	1.86 (2)		

[a] Distances are in angstroms. Estimated standard deviations in the least significant figure are given in parentheses.

Table IV. Intramolecular Bond Angles for 1[a]

Pt(2)–Pt(1)–Ru(1)	93.24 (4)	Pt(1)–Pt(2)–Ru(4)	92.43 (4)
Pt(2)–Pt(1)–Ru(2)	93.23 (4)	Pt(1)–Pt(2)–Ru(5)	59.60 (4)
Pt(2)–Pt(1)–Ru(5)	59.44 (4)	Pt(1)–Pt(2)–Ru(6)	59.27 (4)
Pt(3)–Pt(1)–Ru(6)	59.96 (4)	Pt(1)–Pt(2)–Ru(7)	59.34 (4)
Pt(2)–Pt(1)–Ru(7)	59.66 (4)	Pt(1)–Pt(2)–Ru(8)	60.05 (4)
Pt(2)–Pt(1)–Ru(8)	59.50 (4)	Ru(3)–Pt(2)–Ru(4)	175.59 (5)
Ru(1)–Pt(1)–Ru(2)	172.85 (5)	Ru(3)–Pt(2)–Ru(5)	63.75 (5)
Ru(1)–Pt(1)–Ru(5)	121.05 (5)	Ru(3)–Pt(2)–Ru(6)	120.33 (5)
Ru(1)–Pt(1)–Ru(6)	64.32 (5)	Ru(3)–Pt(2)–Ru(7)	60.85 (5)
Ru(1)–Pt(1)–Ru(7)	119.86 (6)	Ru(3)–Pt(2)–Ru(8)	121.18 (5)
Ru(1)–Pt(1)–Ru(8)	59.76 (5)	Ru(4)–Pt(2)–Ru(5)	120.11 (5)
Ru(2)–Pt(1)–Ru(5)	65.15 (5)	Ru(4)–Pt(2)–Ru(6)	63.57 (5)
Ru(2)–Pt(1)–Ru(6)	121.86 (5)	Ru(4)–Pt(2)–Ru(7)	119.86 (6)
Ru(2)–Pt(1)–Ru(7)	61.42 (5)	Ru(4)–Pt(2)–Ru(8)	59.55 (5)
Ru(2)–Pt(1)–Ru(8)	121.63 (6)	Ru(5)–Pt(2)–Ru(6)	56.58 (5)
Ru(2)–Pt(1)–C(10)	89.4 (6)	Ru(5)–Pt(2)–Ru(7)	91.48 (5)
Ru(5)–Pt(1)–Ru(6)	56.75 (5)	Ru(5)–Pt(2)–Ru(8)	119.55 (5)
Ru(5)–Pt(1)–Ru(7)	91.57 (5)	Ru(6)–Pt(2)–Ru(7)	118.60 (5)
Ru(5)–Pt(1)–Ru(8)	118.84 (5)	Ru(6)–Pt(2)–Ru(8)	89.61 (5)
Ru(6)–Pt(1)–Ru(7)	119.61 (5)	Ru(7)–Pt(2)–Ru(8)	60.37 (5)
Ru(6)–Pt(1)–Ru(8)	89.70 (5)	Ru(7)–C(71)–O(71)	171 (2)
Ru(7)–Pt(1)–Ru(8)	60.29 (5)	Ru(7)–C(72)–O(72)	164 (2)
Pt(1)–Pt(2)–Ru(3)	91.52 (4)	M–C(av)–O	175 (4)

[a] Angles are in degrees. Estimated standard deviations in the least significant figure are given in parentheses.

ruthenium faces Ru(1)–Ru(4)–Ru(6) and Ru(2)–Ru(3)–Ru(5). Triply bridging hydride ligands have been observed recently in other ruthenium complexes[9,17] and were also proposed to occur in the complex $Ru_6(CO)_{18}(\mu_3\text{-}H)_2$.[18] It is well-known that hydride ligands produce a lengthening of the metal–metal bonds that they bridge,[18,19] and it was found that the ruthenium–ruthenium internuclear distances associated with the hydride ligands are uniformly 0.1–0.2 Å longer than those not bridged by the hydrides, 2.915 (2)–3.031 (2) Å vs 2.750 (2)–2.800 (2) Å. A high-field resonance characteristic of hydride ligands was observed in the ^1H NMR spectrum at −15.79 ppm and showed long-range coupling to the platinum atoms, J_{Pt-H} = 22.2 Hz. The molecule contains 23 linear terminal carbonyl ligands distributed as shown in Figure 1, but since Ru(7) contains three carbonyl ligands and Ru(8) has only two, the hydride ligands are inequivalent. The observation of only a single hydride resonance suggests that the structure observed in the solid state may be dynamical in solution and this results in an averaging of the hydride environments. This could be accomplished by a simple exchange of one of the CO ligands on Ru(7) back and forth between Ru(7) and Ru(8). Compound 1 has a total of 132 valence electrons, which is two less the amount expected (134) for

---

[17] McCarthy, D. A.; Krause, J. K.; Shore, S. G. *J. Am. Chem. Soc.* **1990**, *112*, 8587.

[18] Churchill, M. R.; Wormald, J. *J. Am. Chem. Soc.* **1971**, *93*, 5670.

[19] (a) Bau, R. *Struct. Bonding* **1981**, *44*, 1. (b) Churchill, M. R. In *Transition Metal Hydrides*; Advances in Chemistry Series 167; American Chemical Society: Washington, DC, 1978.

Table V. Positional Parameters and *B*(eq) Values (Å^2) for $Pt_3Ru_7(CO)_{22}(\mu_3\text{-}H)_2$, 2

atom	*x*	*y*	*z*	*B*(eq)
Pt(1)	0.21921 (12)	0.09462 (06)	0.75098 (08)	3.03 (7)
Pt(2)	0.49710 (12)	0.12640 (06)	0.75668 (08)	3.03 (7)
Pt(3)	0.31117 (16)	0.20277 (08)	0.82638 (11)	4.0 (1)
Ru(7A)	0.3312	0.2028	0.8264	4.0
Ru(1)	0.1957 (03)	0.10401 (14)	0.90021 (16)	3.8 (2)
Ru(2)	0.2104 (03)	0.9283 (14)	0.60057 (16)	4.0 (2)
Ru(3)	0.5098 (03)	0.12740 (14)	0.60570 (18)	4.3 (2)
Ru(4)	0.4990 (03)	0.13847 (13)	0.90717 (16)	3.9 (2)
Ru(5)	0.4066 (03)	0.01507 (13)	0.68907 (16)	3.7 (1)
Ru(6)	0.3994 (03)	0.02066 (13)	0.83051 (16)	3.6 (1)
Ru(7)	0.31739 (18)	0.19758 (10)	0.67285 (12)	4.5 (1)
Pt(3A)	0.3174	0.1976	0.6728	4.5
O(10)	0.015 (02)	−0.0171 (10)	0.7465 (13)	5 (1)
O(11)	0.035 (02)	−0.0216 (11)	0.9250 (14)	6 (2)
O(12)	0.150 (03)	0.1444 (13)	1.0602 (15)	8 (2)
O(13)	−0.064 (02)	0.1753 (13)	0.8548 (15)	8 (2)
O(20)	0.785 (02)	0.0743 (12)	0.7636 (15)	7 (2)
O(21)	0.183 (03)	0.1270 (14)	0.4390 (18)	9 (2)
O(22)	0.070 (02)	−0.0383 (12)	0.5668 (15)	8 (2)
O(23)	−0.056 (02)	0.1564 (14)	0.6294 (15)	8 (2)
O(30)	0.290 (03)	0.2896 (12)	0.9546 (13)	7 (2)
O(31)	0.701 (02)	0.2415 (12)	0.6507 (15)	7 (2)
O(32)	0.750 (02)	0.0397 (13)	0.5712 (19)	10 (2)
O(33)	0.491 (03)	0.1663 (18)	0.4475 (17)	11 (2)
O(41)	0.744 (02)	0.0605 (13)	0.9587 (14)	8 (2)
O(42)	0.471 (02)	0.1903 (14)	1.0604 (16)	8 (2)
O(43)	0.681 (02)	0.2516 (12)	0.8634 (15)	7 (2)
O(51)	0.658 (02)	−0.0673 (14)	0.6836 (16)	9 (2)
O(52)	0.262 (02)	−0.1136 (11)	0.6727 (15)	7 (2)
O(61)	0.652 (03)	−0.0564 (14)	0.8640 (18)	9 (2)
O(62)	0.259 (02)	−0.1075 (11)	0.8575 (15)	7 (2)
O(70)	0.291 (02)	0.2748 (13)	0.5361 (13)	7 (2)
O(71)	0.491 (02)	0.3213 (11)	0.7445 (18)	8 (2)
O(72)	0.050 (02)	0.2755 (12)	0.7384 (16)	8 (2)
C(10)	0.094 (03)	0.0239 (15)	0.7507 (17)	3.6 (7)
C(11)	0.096 (03)	0.0245 (16)	0.9184 (17)	3.4 (7)
C(12)	0.170 (03)	0.1291 (17)	1.002 (02)	4.9 (8)
C(13)	0.033 (04)	0.1490 (16)	0.8708 (19)	4.3 (8)
C(20)	0.678 (04)	0.0921 (16)	0.7636 (19)	4.6 (8)
C(21)	0.192 (04)	0.113 (02)	0.498 (03)	7 (1)
C(22)	0.126 (03)	0.0095 (18)	0.5763 (18)	4.5 (8)
C(23)	0.046 (04)	0.1366 (18)	0.621 (02)	5.1 (9)
C(30)	0.290 (03)	0.2577 (16)	0.9047 (20)	4.0 (8)
C(31)	0.627 (03)	0.2010 (16)	0.6340 (18)	4.0 (7)
C(32)	0.657 (04)	0.0696 (17)	0.5831 (19)	4.9 (8)
C(33)	0.492 (04)	0.147 (02)	0.508 (03)	7 (1)
C(41)	0.648 (03)	0.0868 (16)	0.9406 (19)	4.3 (8)
C(42)	0.478 (04)	0.1679 (20)	1.006 (03)	6 (1)
C(43)	0.610 (03)	0.2085 (16)	0.8766 (17)	3.6 (7)
C(51)	0.563 (04)	−0.0357 (19)	0.682 (02)	6 (1)
C(52)	0.311 (03)	−0.0616 (18)	0.6760 (18)	4.3 (8)
C(61)	0.558 (04)	−0.0261 (19)	0.856 (02)	5.4 (9)
C(62)	0.309 (03)	−0.0591 (16)	0.8499 (17)	3.5 (7)
C(70)	0.303 (03)	0.2439 (16)	0.589 (02)	4.4 (8)
C(71)	0.424 (05)	0.276 (03)	0.740 (03)	10 (1)
C(72)	0.150 (05)	0.249 (03)	0.727 (03)	11 (1)

two edge-shared octahedra having bonds between both apical pairs of metal atoms,[16,20] and it is believed that the unusual shortness of the Ru(5)–Ru(6) bond may be a result of this electronic unsaturation.

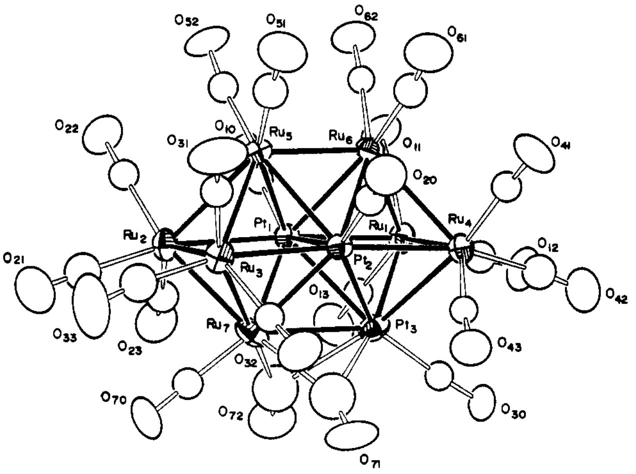

Figure 2. ORTEP diagram of $Ru_7Pt_3(CO)_{22}(\mu_3\text{-}H)_2$, **2**, showing 50% probability thermal ellipsoids.

Table VI. Intramolecular Distances for 2[a]

Pt(1)–Pt(2)	2.808 (2)	Pt(3)–C(72)	2.56 (5)
Pt(1)–Pt(3)	2.731 (2)	Ru(1)–Ru(4)	3.064 (4)
Pt(1)–Ru(1)	2.753 (4)	Ru(1)–Ru(6)	2.937 (4)
Pt(1)–Ru(2)	2.752 (4)	Ru(2)–Ru(3)	3.027 (4)
Pt(1)–Ru(5)	2.718 (3)	Ru(2)–Ru(5)	2.945 (4)
Pt(1)–Ru(6)	2.715 (3)	Ru(2)–Ru(7)	2.700 (4)
Pt(1)–Ru(7)	2.720 (2)	Ru(3)–Ru(5)	2.936 (4)
Pt(2)–Pt(3)	2.736 (2)	Ru(3)–Ru(7)	2.690 (4)
Pt(2)–Ru(3)	2.769 (4)	Ru(4)–Ru(6)	2.925 (4)
Pt(2)–Ru(4)	2.764 (4)	Ru(5)–Ru(6)	2.593 (5)
Pt(2)–Ru(5)	2.712 (3)	Ru(7)–C(71)	2.25 (5)
Pt(2)–Ru(6)	2.721 (3)	Ru(7)–C(72)	2.20 (6)
Pt(2)–Ru(7)	2.724 (2)	Ru(1)–Ru(4)	3.064 (4)
Pt(3)–Ru(1)	2.683 (4)	Ru(2)–Ru(3)	3.027 (4)
Pt(3)–Ru(4)	2.675 (3)	M–C(av)	1.88 (4)
Pt(3)–Ru(7)	2.814 (3)	O–C(av)	1.13 (5)
Pt(3)–C(71)	2.45 (6)		

[a] Distances are in angstroms. Estimated standard deviations in the least significant figure are given in parentheses.

Table VII. Intramolecular Bond Angles for 2[a]

Pt(2)–Pt(1)–Ru(1)	93.09 (7)	Ru(1)–Pt(3)–Ru(7)	119.7 (1)
Pt(2)–Pt(1)–Ru(2)	92.63 (8)	Ru(4)–Pt(3)–Ru(7)	120.1 (1)
Pt(3)–Pt(1)–Ru(2)	121.2 (1)	Pt(3)–Ru(1)–Ru(6)	84.7 (1)
Pt(3)–Pt(1)–Ru(5)	117.84 (8)	Ru(5)–Ru(2)–Ru(7)	84.8 (1)
Pt(3)–Pt(1)–Ru(6)	88.21 (8)	Ru(5)–Ru(3)–Ru(7)	85.1 (1)
Ru(1)–Pt(1)–Ru(2)	172.6 (1)	Pt(3)–Ru(4)–Ru(6)	85.1 (1)
Ru(1)–Pt(1)–Ru(5)	122.0 (1)	Pt(1)–Ru(5)–Ru(3)	90.2 (1)
Ru(1)–Pt(1)–Ru(7)	120.6 (1)	Pt(2)–Ru(5)–Ru(2)	90.5 (1)
Ru(2)–Pt(1)–Ru(6)	122.2 (1)	Ru(2)–Ru(5)–Ru(6)	119.4 (1)
Ru(5)–Pt(1)–Ru(7)	88.97 (9)	Ru(3)–Ru(5)–Ru(6)	120.2 (1)
Ru(6)–Pt(1)–Ru(7)	117.98 (8)	Pt(1)–Ru(6)–Ru(4)	90.7 (1)
Pt(1)–Pt(2)–Ru(3)	91.92 (8)	Pt(2)–Ru(6)–Ru(1)	90.9 (1)
Pt(1)–Pt(2)–Ru(4)	92.24 (8)	Ru(1)–Ru(6)–Ru(5)	119.7 (1)
Pt(3)–Pt(2)–Ru(3)	120.59 (9)	Ru(4)–Ru(6)–Ru(5)	119.8 (1)
Pt(3)–Pt(2)–Ru(5)	117.87 (8)	Pt(1)–Ru(7)–Ru(3)	95.6 (1)
Pt(3)–Pt(2)–Ru(6)	87.99 (8)	Pt(2)–Ru(7)–Ru(2)	95.68 (9)
Ru(3)–Pt(2)–Ru(4)	173.7 (1)	Pt(3)–Ru(7)–Ru(2)	120.0 (1)
Ru(3)–Pt(2)–Ru(6)	121.8 (1)	Pt(3)–Ru(7)–Ru(3)	120.6 (1)
Ru(4)–Pt(2)–Ru(5)	121.5 (1)	Pt(3)–C(71)–O(71)	136 (4)
Ru(4)–Pt(2)–Ru(7)	120.1 (1)	Pt(3)–C(72)–O(72)	123 (4)
Ru(5)–Pt(2)–Ru(7)	89.01 (8)	Ru(7)–C(71)–O(71)	151 (5)
Ru(6)–Pt(2)–Ru(7)	117.65 (8)	Ru(7)–C(72)–O(72)	163 (4)
Pt(1)–Pt(3)–Ru(4)	95.95 (9)	M–C(av)–O	175 (4)
Pt(2)–Pt(3)–Ru(1)	96.30 (9)		

[a] Angles are in degrees. Estimated standard deviations in the least significant figure are given in parentheses.

An ORTEP diagram of the structure of 2 is shown in Figure 2. Final atom positional parameters are listed in Table V. Selected interatomic distances and angles are listed in Tables VI and VII. The molecule consists of a cluster of two edge-fused bioctahedra similar to that of 1. The Pt–Pt bond distance between the platinum atoms at the edge-sharing site is slightly longer than that in 1, 2.808 (2) Å. The third platinum atom Pt(3) occupies one of the apical sites. The solid-state structure exhibited a disorder such that the platinum Pt(3) possessed 50% occupancy in the site shown by Ru(7) in Figure 2. Two carbonyl ligands bridge the Pt(3)–Ru(7) bond with one terminal ligand on each metal atom. The remainder of the CO

---

(20) Mingos, D. M. P.; May, A. S. In *The Chemistry of Metal Cluster Complexes*; Shriver, D. F., Kaesz, H. D., Adams, R. D., Eds.; VCH Publishers: New York, 1990; Chapter 2.

Table VIII. Positional Parameters and B(eq) Values (Å^2) for 3

atom	x	y	z	B(eq)
Pt(1)	0.83383 (05)	0.20599 (03)	0.921481 (20)	2.72 (3)
Pt(2)	1.02805 (05)	0.23775 (03)	0.875305 (20)	2.79 (3)
Ru(1)	0.97901 (12)	0.14612 (06)	0.99362 (04)	3.46 (6)
Ru(2)	0.99108 (12)	0.10594 (06)	0.89430 (04)	3.66 (6)
Ru(3)	1.20420 (12)	0.18402 (06)	0.94029 (04)	3.52 (6)
Ru(4)	1.02712 (11)	0.27510 (05)	0.96949 (04)	2.98 (6)
Ru(5)	0.78696 (11)	0.33238 (06)	0.94830 (04)	3.07 (6)
Ru(6)	1.00432 (11)	0.36820 (06)	0.89819 (04)	3.14 (6)
Ru(7)	0.79530 (11)	0.29893 (05)	0.85167 (04)	2.82 (6)
Ru(8)	0.64470 (12)	0.40445 (06)	0.80048 (04)	3.12 (6)
Cl(1)	0.4892 (09)	0.0562 (05)	0.5299 (04)	19.0 (9)
Cl(2)	0.5612 (16)	0.0059 (06)	0.0408 (05)	13 (1)
P(1)	0.6966 (04)	0.40360 (19)	0.72382 (14)	3.4 (2)
P(2)	0.5671 (04)	0.50820 (19)	0.78376 (15)	3.7 (2)
O(10)	0.5860 (12)	0.1518 (07)	0.9509 (05)	7.7 (8)
O(11)	0.7905 (13)	0.1945 (07)	1.0612 (05)	7.8 (8)
O(12)	0.8354 (13)	0.0191 (06)	0.9866 (04)	6.4 (7)
O(13)	1.1521 (12)	0.0965 (06)	1.0766 (04)	6.0 (7)
O(20)	1.2373 (12)	0.2460 (06)	0.8075 (04)	6.7 (7)
O(21)	0.7267 (12)	0.0575 (08)	0.8645 (05)	9 (1)
O(22)	1.1065 (12)	−0.0290 (05)	0.8973 (04)	6.5 (7)
O(23)	1.0456 (13)	0.1103 (06)	0.7917 (05)	6.9 (8)
O(31)	1.3817 (11)	0.2954 (06)	0.9211 (05)	6.8 (8)
O(32)	1.3354 (11)	0.1060 (06)	0.8690 (04)	6.0 (7)
O(33)	1.3867 (12)	0.1359 (08)	1.0201 (04)	8.6 (9)
O(41)	1.1987 (11)	0.2518 (05)	1.0577 (04)	5.8 (7)
O(42)	1.2078 (12)	0.3855 (05)	0.9844 (04)	6.1 (7)
O(43)	0.9103 (10)	0.3361 (06)	1.0533 (04)	5.5 (6)
O(51)	0.5733 (12)	0.2878 (06)	1.0084 (04)	6.4 (7)
O(52)	0.7778 (13)	0.4686 (06)	0.9862 (05)	8.0 (8)
O(53)	0.6079 (09)	0.4016 (05)	0.8771 (03)	3.6 (5)
O(61)	1.2385 (13)	0.3935 (06)	0.8453 (05)	7.8 (8)
O(62)	1.0060 (12)	0.5061 (06)	0.9316 (04)	6.7 (7)
O(63)	0.8308 (09)	0.4390 (04)	0.8264 (03)	3.4 (5)
O(71)	0.5844 (13)	0.1974 (06)	0.8363 (04)	7.4 (8)
O(72)	0.9145 (10)	0.2406 (05)	0.7668 (04)	5.3 (6)
O(81)	0.3917 (11)	0.3500 (06)	0.7674 (04)	6.1 (7)
C(1)	0.5494 (16)	0.5141 (07)	0.7204 (05)	4.5 (8)
C(2)	0.6640 (15)	0.4832 (07)	0.6985 (05)	4.2 (8)
C(10)	0.6790 (16)	0.1722 (08)	0.9406 (06)	4.2 (9)
C(11)	0.8625 (17)	0.1781 (08)	1.0349 (06)	5 (1)
C(12)	0.8922 (16)	0.0667 (08)	0.9858 (05)	4.1 (9)
C(13)	1.0916 (16)	0.1148 (07)	1.0457 (05)	3.6 (8)
C(20)	1.1595 (16)	0.2453 (07)	0.8335 (06)	4.3 (9)
C(21)	0.8235 (18)	0.0785 (11)	0.8784 (07)	7 (1)
C(22)	1.0619 (15)	0.0204 (08)	0.8972 (05)	3.9 (8)
C(23)	1.0256 (17)	0.1143 (08)	0.8308 (07)	5 (1)
C(31)	1.3128 (14)	0.2557 (08)	0.9289 (06)	4.3 (9)
C(32)	1.2829 (14)	0.1322 (08)	0.8959 (06)	3.9 (8)
C(33)	1.3182 (16)	0.1547 (09)	0.9907 (06)	5 (1)
C(41)	1.1329 (17)	0.2534 (08)	1.0230 (06)	4.6 (9)
C(42)	1.1285 (16)	0.3531 (07)	0.9666 (06)	4.2 (8)
C(43)	0.9195 (14)	0.3190 (07)	1.0145 (05)	3.5 (8)
C(51)	0.6522 (15)	0.3020 (07)	0.9854 (05)	3.8 (8)
C(52)	0.7794 (16)	0.4180 (08)	0.9699 (06)	5 (1)
C(53)	0.6825 (15)	0.3604 (07)	0.8921 (05)	3.5 (8)
C(61)	1.1515 (17)	0.3814 (07)	0.8663 (06)	4.5 (9)
C(62)	1.0057 (15)	0.4546 (08)	0.9202 (06)	4.3 (9)
C(63)	0.8800 (14)	0.3927 (07)	0.8482 (05)	3.1 (7)
C(71)	0.6735 (17)	0.2310 (08)	0.8464 (05)	4.4 (9)
C(72)	0.8894 (14)	0.2587 (07)	0.8042 (05)	3.5 (8)
C(81)	0.4896 (15)	0.3704 (08)	0.7813 (05)	3.8 (8)

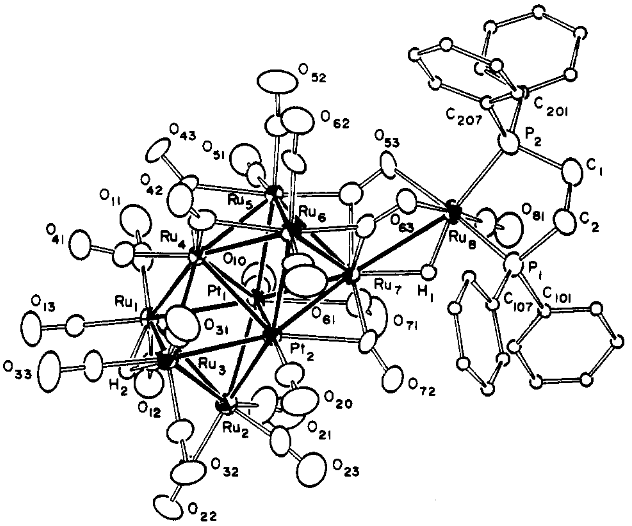

Figure 3. ORTEP diagram of $Ru_8Pt_2(CO)_{21}(\mu_3\text{-}CO)_2(dppe)(\mu\text{-}H)_2$, 3, showing 50% probability thermal ellipsoids.

Table IX. Intramolecular Distances for 3[a]

Pt(1)–Pt(2)	2.5914 (9)	Ru(4)–C(42)	1.94 (2)
Pt(1)–Ru(1)	2.752 (1)	Ru(4)–C(43)	1.99 (1)
Pt(1)–Ru(2)	2.791 (1)	Ru(5)–Ru(6)	2.877 (2)
Pt(1)–Ru(4)	2.756 (1)	Ru(5)–Ru(7)	2.836 (2)
Pt(1)–Ru(5)	2.774 (1)	Ru(5)–C(43)	2.27 (2)
Pt(1)–Ru(7)	2.767 (1)	Ru(5)–C(51)	1.93 (2)
Pt(1)–C(10)	1.89 (2)	Ru(5)–C(52)	1.88 (2)
Pt(1)–C(71)	2.66 (2)	Ru(5)–C(53)	1.95 (2)
Pt(2)–Ru(2)	2.809 (1)	Ru(6)–Ru(7)	2.858 (2)
Pt(2)–Ru(3)	2.745 (1)	Ru(6)–C(42)	2.28 (2)
Pt(2)–Ru(4)	2.783 (1)	Ru(6)–C(61)	1.87 (2)
Pt(2)–Ru(6)	2.788 (1)	Ru(6)–C(62)	1.89 (2)
Pt(2)–Ru(7)	2.788 (1)	Ru(6)–C(63)	1.92 (1)
Pt(2)–C(20)	1.89 (2)	Ru(7)–Ru(8)	3.002 (2)
Pt(2)–C(72)	2.44 (1)	Ru(7)–C(53)	2.13 (1)
Ru(1)–Ru(2)	2.950 (2)	Ru(7)–C(63)	2.14 (1)
Ru(1)–Ru(3)	3.007 (2)	Ru(7)–C(71)	1.90 (2)
Ru(1)–Ru(4)	2.807 (2)	Ru(7)–C(72)	1.92 (2)
Ru(1)–C(11)	1.88 (2)	Ru(7)–H(1)	1.9 (1)
Ru(1)–C(12)	1.88 (2)	Ru(8)–P(1)	2.283 (4)
Ru(1)–C(13)	1.93 (2)	Ru(8)–P(2)	2.329 (4)
Ru(1)–H(2)	1.9 (1)	Ru(8)–O(53)	2.24 (1)
Ru(2)–Ru(3)	2.979 (2)	Ru(8)–O(63)	2.16 (1)
Ru(2)–C(21)	1.87 (2)	Ru(8)–C(81)	1.82 (2)
Ru(2)–C(22)	1.92 (2)	Ru(8)–H(1)	1.6 (1)
Ru(2)–C(23)	1.87 (2)	P(1)–C(2)	1.82 (1)
Ru(3)–Ru(4)	2.815 (2)	P(1)–C(101)	1.82 (2)
Ru(3)–C(31)	1.91 (2)	P(1)–C(107)	1.81 (2)
Ru(3)–C(32)	1.89 (2)	P(2)–C(1)	1.80 (2)
Ru(3)–C(33)	1.89 (2)	P(2)–C(201)	1.80 (2)
Ru(3)–H(2)	1.9 (1)	P(2)–C(207)	1.82 (1)
Ru(4)–Ru(5)	2.810 (2)	C(1)–C(2)	1.53 (2)
Ru(4)–Ru(6)	2.789 (2)	O–C(av)	1.15 (3)
Ru(4)–C(41)	1.87 (2)		

[a] Distances are in angstroms. Estimated standard deviations in the least significant figure are given in parentheses.

ligand distribution is analogous to that found in 1. The Ru(5)–Ru(6) distance is also unusually short, 2.593 (5) Å, as found in 1. The ^1H NMR spectrum indicated the presence of two inequivalent hydride ligands which show long-range coupling to each other and to platinum, δ = −9.83 (d, J_{Pt-H} = 24.7 Hz, J_{H-H} = 1.0 Hz), −19.56 (d, J_{Pt-H} = 19.2 Hz, J_{H-H} = 1.0 Hz). Due to the disorder the quality of the structure of 2 was not quite as good as that of 1 and the hydride ligands could not be located directly in the structural analysis. They are, however, believed to occupy triply bridging sites on the triruthenium faces Ru(1)–Ru(4)–Ru(6) and Ru(2)–Ru(3)–Ru(5) just as observed in 1. The Ru–Ru distances of these triangles are also significantly longer than the others. Like 1, compound 2 is also electron deficient by the amount of two electrons, and the short Ru(5)–Ru(6) bond distance may be a consequence of this.

Anticipating that the electronic unsaturation would result in increased reactivity toward the addition of nucleophiles, it was decided to study the reactions of 1 and 2 with CO and 1 with dppe. Only one complex could be isolated and characterized from the reaction of 1 with dppe. It was identified as the adduct $Ru_8Pt_2(CO)_{21}(\mu_3\text{-}CO)_2(dppe)(\mu\text{-}H)_2$, 3, 12% yield. Compound 3 was char-

Table X. Intramolecular Bond Angles for 3[a]

Pt(2)–Pt(1)–Ru(1)	94.42 (4)	P(2)–Ru(8)–O(53)	98.0 (3)
Pt(2)–Pt(1)–Ru(5)	93.63 (3)	P(2)–Ru(8)–O(63)	93.4 (3)
Ru(1)–Pt(1)–Ru(5)	108.59 (4)	O(53)–Ru(8)–O(63)	84.0 (3)
Ru(1)–Pt(1)–Ru(7)	152.55 (4)	Ru(8)–P(1)–C(2)	108.6 (5)
Ru(2)–Pt(1)–Ru(4)	95.23 (4)	Ru(8)–P(2)–C(1)	105.9 (5)
Ru(2)–Pt(1)–Ru(5)	153.37 (4)	P(2)–C(1)–C(2)	111 (1)
Ru(2)–Pt(1)–Ru(7)	111.93 (4)	P(1)–C(2)–C(1)	110 (1)
Ru(4)–Pt(1)–Ru(7)	93.24 (4)	Ru(4)–C(42)–O(42)	148 (1)
Pt(1)–Pt(2)–Ru(3)	94.25 (4)	Ru(6)–C(42)–O(42)	130 (1)
Pt(1)–Pt(2)–Ru(6)	92.25 (3)	Ru(4)–C(43)–O(43)	147 (1)
Ru(2)–Pt(2)–Ru(4)	94.24 (4)	Ru(5)–C(43)–O(43)	131 (1)
Ru(2)–Pt(2)–Ru(6)	151.22 (4)	Ru(5)–C(53)–O(53)	143 (1)
Ru(2)–Pt(2)–Ru(7)	110.75 (4)	Ru(7)–C(53)–O(53)	127 (1)
Ru(3)–Pt(2)–Ru(6)	107.57 (4)	Ru(6)–C(63)–O(63)	144 (1)
Ru(3)–Pt(2)–Ru(7)	151.48 (4)	Ru(7)–C(63)–O(63)	125 (1)
Ru(4)–Pt(2)–Ru(7)	92.19 (4)	Ru(7)–C(71)–O(71)	166 (1)
P(1)–Ru(8)–P(2)	85.3 (1)	Pt(2)–C(72)–O(72)	122 (1)
P(1)–Ru(8)–O(53)	175.7 (3)	Ru(7)–C(72)–O(72)	159 (1)
P(1)–Ru(8)–O(63)	93.0 (3)	M–C(av)–O	176 (2)

[a] Angles are in degrees. Estimated standard deviations in the least significant figure are given in parentheses.

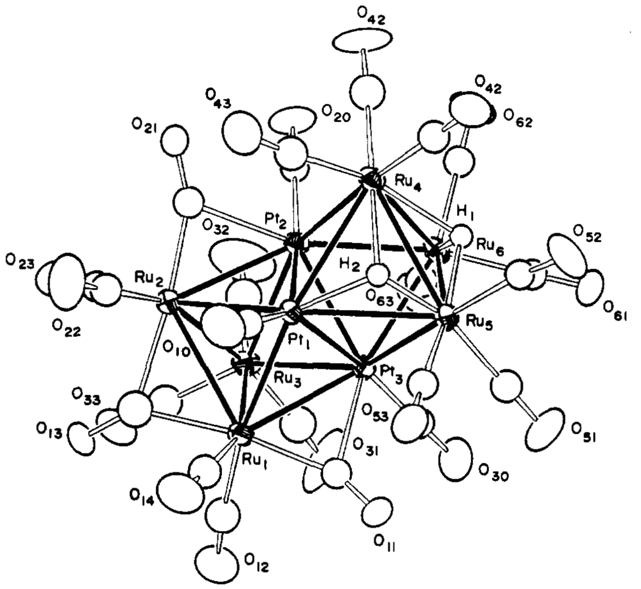

Figure 4. ORTEP diagram of $Ru_6Pt_3(CO)_{21}(\mu\text{-}CO)(\mu\text{-}H)_2$, 4, showing 50% probability thermal ellipsoids.

acterized structurally by X-ray diffraction, and an ORTEP diagram of the molecular structure of 3 is shown in Figure 3. Final atom positional parameters are listed in Table VIII. Selected interatomic distances and angles are listed in Tables IX and X. The molecule consists of a cluster of nine metal atoms arranged in the form of two face-shared bioctahedra. The two platinum atoms lie in the shared face, and the Pt–Pt bond distance has shortened to 2.5914 (9) Å, a value typical of the bond distances in Pt_3 triangles.[7,9,10,14] The tenth metal atom contains the dppe ligand and extends from one of the Ru_3 triangles as a "spike". It is linked to the cluster by the hydride-bridged metal–metal bond Ru(7)–Ru(8), 3.002 (2) Å. Most interestingly, this connection is also bridged by two novel μ_3-η^2-bridging carbonyl ligands. The carbon atoms of these ligands bridge two adjacent Ru–Ru bonds in the Ru_3 triangle of the cluster, and the oxygen atoms are coordinated to the external metal atom Ru(8), Ru(8)–O(53) = 2.24 (1) Å and Ru(8)–O(63) = 2.16 (1) Å. The distances between Ru(8) and the carbon atoms are so long that it is unlikely that there is any significant bonding between them, Ru(8)···C(53) = 2.75 (1) Å and Ru(8)···C(63) = 2.74 (1) Å. The C–O distances are slightly longer than those of terminal CO ligands, C(53)–O(53) = 1.21 (2) Å and C(63)–O(63) = 1.23 (2) Å, which is indicative of a greater reduction of the CO bond order. The reduction of the CO bond order was also indicated by the low frequency of the CO stretching vibration of 1612 cm^{-1}. The identification of this assignment was confirmed by the preparation of a ^{13}CO-enriched sample of 3 for which the absorption was observed shifted to 1568 cm^{-1}. Compound 3 contains two bridging hydride ligands. Both were observed crystallographically. One bridges the Ru(7)–Ru(8) bond and shows coupling to both phosphorus atoms of the dppe ligand, $\delta = -7.70$ (dd, 1H, $J_{P-H}(cis) = 10$ Hz, $J_{P-H}(trans) = 29$ Hz). The other H(2) bridges the elongated Ru(1)–Ru(3) bond on the other side of the cluster, $\delta = -18.09$ (s, 1H). This molecule is dynamically active in solution, and the positions of the hydride resonances were obtained from a spectrum recorded at −57 °C.

Table XI. Metal and Hydride Ligand Positional Parameters and B(eq) Values (Å^2) for $Pt_3Ru_6(CO)_{21}(\mu\text{-}CO)(\mu_3\text{-}H)_2$, 4

atom	x	y	z	B(eq)
Pt(1A)	0.43491 (04)	0.18779 (05)	0.68147 (04)	2.30 (3)
Pt(1B)	0.79061 (04)	0.22933 (05)	0.17336 (04)	2.29 (3)
Pt(2A)	0.39386 (04)	0.33309 (05)	0.62880 (04)	2.34 (3)
Pt(2B)	0.91070 (04)	0.15394 (05)	0.24364 (04)	2.28 (3)
Pt(3A)	0.29900 (04)	0.21266 (05)	0.60483 (04)	2.29 (3)
Pt(3B)	0.90320 (04)	0.31849 (05)	0.24328 (04)	2.24 (3)
Ru(1A)	0.34878 (09)	0.18364 (11)	0.74231 (08)	2.71 (7)
Ru(1B)	0.84124 (09)	0.32297 (10)	0.10302 (08)	2.57 (7)
Ru(2A)	0.44790 (09)	0.31258 (11)	0.76851 (08)	2.78 (7)
Ru(2B)	0.84772 (10)	0.14940 (11)	0.10233 (08)	2.86 (8)
Ru(3A)	0.29944 (10)	0.34115 (11)	0.68610 (08)	2.86 (7)
Ru(3B)	0.97435 (09)	0.24018 (11)	0.17898 (08)	2.59 (7)
Ru(4A)	0.46769 (09)	0.24424 (11)	0.57523 (08)	2.65 (7)
Ru(4B)	0.81232 (10)	0.13941 (11)	0.29424 (08)	2.89 (8)
Ru(5A)	0.36331 (10)	0.11437 (10)	0.54800 (08)	2.59 (7)
Ru(5B)	0.80310 (09)	0.31722 (10)	0.29098 (08)	2.74 (7)
Ru(6A)	0.31235 (09)	0.28290 (11)	0.50070 (08)	2.66 (7)
Ru(6B)	0.94591 (09)	0.23463 (11)	0.36021 (08)	2.78 (7)
H(1A)	0.377 (09)	0.192 (10)	0.504 (08)	4.0
H(2A)	0.449 (09)	0.130 (10)	0.610 (08)	4.0
H(1B)	0.846 (09)	0.226 (10)	0.349 (08)	4.0
H(2B)	0.757 (09)	0.225 (10)	0.220 (08)	4.0

1 and 2 both react with CO at 25 °C to yield brown products of high metal nuclearity, but only the product obtained from the reaction of 2, $Ru_6Pt_3(CO)_{21}(\mu\text{-}CO)(\mu_3\text{-}H)_2$ (4; 55% yield), could be fully characterized by single-crystal X-ray diffraction analysis. An ORTEP diagram of the structure of 4 is shown in Figure 4. Final atom positional

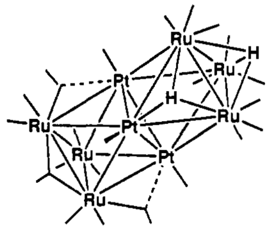

4

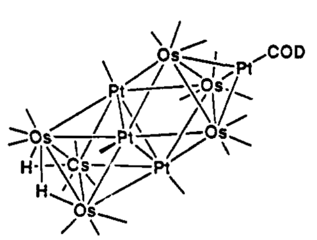

5

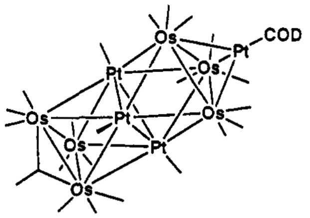

6

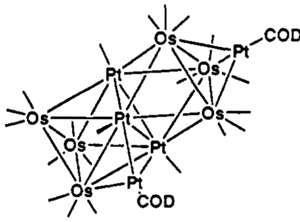

7

Table XII. Intramolecular Distances for Molecule A of 4[a]

Pt(1A)-Pt(2A)	2.645 (1)	Pt(3A)-Ru(6A)	2.726 (2)
Pt(1A)-Pt(3A)	2.647 (1)	Pt(3A)-C(11A)	2.40 (2)
Pt(1A)-Ru(1A)	2.734 (2)	Ru(1A)-Ru(2A)	2.870 (3)
Pt(1A)-Ru(2A)	2.761 (2)	Ru(1A)-Ru(3A)	2.877 (3)
Pt(1A)-Ru(4A)	2.912 (2)	Ru(2A)-Ru(3A)	2.891 (3)
Pt(1A)-Ru(5A)	2.927 (2)	Ru(4A)-Ru(5A)	2.952 (3)
Pt(1A)-H(2A)	2.0 (2)	Ru(4A)-Ru(6A)	3.026 (2)
Pt(2A)-Pt(3A)	2.714 (1)	Ru(4A)-H(1A)	2.1 (2)
Pt(2A)-Ru(2A)	2.814 (2)	Ru(4A)-H(2A)	2.1 (2)
Pt(2A)-Ru(3A)	2.834 (2)	Ru(5A)-Ru(6A)	3.005 (3)
Pt(2A)-Ru(4A)	2.787 (2)	Ru(5A)-H(1A)	1.7 (2)
Pt(2A)-Ru(6A)	2.718 (2)	Ru(5A)-H(2A)	1.7 (2)
Pt(2A)-C(21A)	2.34 (2)	Ru(6A)-H(1A)	2.0 (2)
Pt(3A)-Ru(1A)	2.798 (2)	Pt-C(av)	1.87 (3)
Pt(3A)-Ru(3A)	2.792 (2)	Ru-C(av)	1.91 (3)
Pt(3A)-Ru(5A)	2.776 (2)	O-C(av)	1.14 (3)

[a] Distances are in angstroms. Estimated standard deviations in the least significant figure are given in parentheses.

parameters are listed in Table XI. Selected interatomic distances and angles are listed in Tables XII and XIII. The complex crystallizes with two crystallographically independent molecules in the asymmetric crystal unit. Both molecules are structurally similar and consist of a cluster of nine metal atoms arranged into three trinuclear layers of pure ruthenium and pure platinum. The cluster could also be described as two face-shared bioctahedra sharing a Pt_3 face. The arrangement of metals is analogous to the platinum–osmium cluster complexes $Os_6Pt_4(CO)_{21}(COD)(\mu_2\text{-}H)_2$, 5,[7] $Os_6Pt_4(CO)_{22}(COD)$, 6,[10] and $Os_6Pt_5(CO)_{21}(COD)_2$, 7,[10] that we have recently reported. These clusters also contain Pt(COD) capping groups on selected triangular metal faces.

The Pt–Pt bond distances in 4, 2.634 (1)–2.727 (1) Å, are similar to the distances observed in the Pt_3 triangles in 5–7, 2.609 (1)–2.690 (1) Å.[7,10] Each platinum atom contains one linear terminal carbonyl ligand. There is a symmetrical bridging carbonyl ligand across the Ru(1)–Ru(2) metal–metal bond and one carbonyl ligand on Ru(1), C(11)–O(11), and one on Ru(2), C(21)–O(21), is a semibridging ligand to a neighboring platinum atom. Each molecule has two triply bridging hydride ligands that were located and refined crystallographically. One, H(1), is a triple bridge across a Ru_3 triangle. The other, H(2), bridges a combination of two ruthenium atoms and one platinum atom. As expected the metal–metal bonds associated with the bridging hydride ligands are longer than the others. In the ^1H NMR spectrum only one hydride resonance was

Scheme I

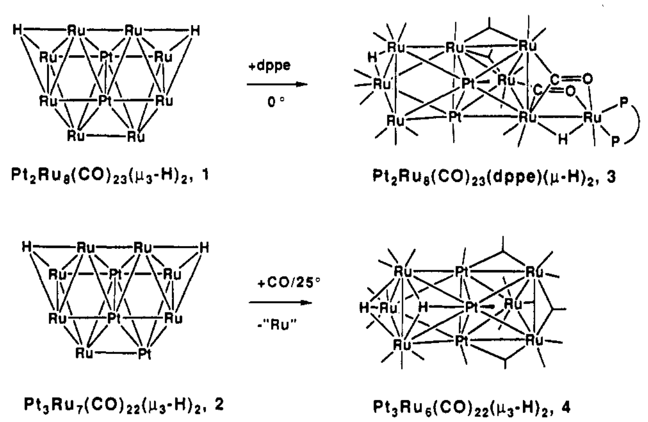

$Pt_2Ru_8(CO)_{23}(\mu_3\text{-}H)_2$, 1

$Pt_2Ru_8(CO)_{23}(dppe)(\mu\text{-}H)_2$, 3

$Pt_3Ru_7(CO)_{22}(\mu_3\text{-}H)_2$, 2

$Pt_3Ru_6(CO)_{22}(\mu_3\text{-}H)_2$, 4

observed at 25 °C, $\delta = -17.19$ (s, 2H, $J_{Pt-H} = 17.0$ Hz) possibly due to dynamical averaging. Efforts to observe the separate resonances by cooling to −97 °C were unsuccessful, and no hydride resonance was observed at this temperature. Compound 4 contains a total of 124 valence electrons and is in accord with the prediction of the skeletal electron pair theory for two face-shared octahedra.[20] Without additional evidence it is not possible to predict exactly what the structure or formula of the product of the reaction of 1 with CO is, but we suspect that it is probably a nine-metal cluster complex similar to 4.

Discussion

In previous studies we have shown that the tetraruthenium cluster complex $Ru_4(CO)_{13}(\mu\text{-}H)_2$ reacts with $Pt(COD)_2$ to yield the mixed-metal cluster complexes $Ru_4Pt(CO)_{13}(COD)(\mu\text{-}H)_2$, $Ru_3Pt(CO)_{10}(COD)(\mu\text{-}H)_2$, $Ru_4Pt_2(CO)_{11}(COD)_2(\mu_3\text{-}H)_2$, and $Ru_5Pt_5(CO)_{18}(COD)_2(\mu_3\text{-}H)_2$ with the latter two in very low yields.[9] In this study we have found that both tetranuclear cluster complexes $Ru_4(CO)_{13}(\mu\text{-}H)_2$ and $Ru_3Pt(CO)_{10}(COD)(\mu\text{-}H)_2$ will combine with the hexanuclear platinum–ruthenium complex $Ru_4Pt_2(CO)_{18}$ to yield the decanuclear products 1 and 2, which possess edge-fused bioctahedral cluster with platinum atoms at the edge-shared sites. Both complexes are formally electronically unsaturated and readily add donor ligands at 25 °C, dppe to 1 and CO to 2, to yield the products 3 and 4, respectively, in a process that leads to a transformation of the clusters into a nine-metal group having the form of two face-shared bioctahedra; see

Table XIII. Intramolecular Bond Angles for Molecule A of 4[a]

Pt(2A)-Pt(1A)-Ru(1A)	94.71 (5)	Ru(1A)-Pt(3A)-Ru(6A)	150.96 (6)
Pt(2A)-Pt(1A)-Ru(5A)	90.54 (5)	Ru(3A)-Pt(3A)-Ru(5A)	152.35 (6)
Pt(3A)-Pt(1A)-Ru(2A)	94.05 (5)	Ru(3A)-Pt(3A)-Ru(6A)	104.97 (6)
Pt(3A)-Pt(1A)-Ru(4A)	91.11 (5)	Pt(1A)-Ru(1A)-Ru(3A)	87.47 (6)
Ru(1A)-Pt(1A)-Ru(4A)	151.02 (6)	Pt(3A)-Ru(1A)-Ru(2A)	88.57 (6)
Ru(1A)-Pt(1A)-Ru(5A)	109.69 (6)	Pt(1A)-Ru(2A)-Ru(3A)	86.68 (6)
Ru(2A)-Pt(1A)-Ru(4A)	110.39 (6)	Pt(2A)-Ru(2A)-Ru(1A)	88.24 (6)
Ru(2A)-Pt(1A)-Ru(5A)	150.05 (6)	Pt(2A)-Ru(3A)-Ru(1A)	87.71 (6)
Pt(1A)-Pt(2A)-Ru(3A)	90.11 (5)	Pt(3A)-Ru(3A)-Ru(2A)	88.27 (6)
Pt(1A)-Pt(2A)-Ru(6A)	96.63 (5)	Pt(1A)-Ru(4A)-Ru(6A)	84.81 (6)
Pt(3A)-Pt(2A)-Ru(2A)	91.43 (5)	Pt(2A)-Ru(4A)-Ru(5A)	87.31 (6)
Pt(3A)-Pt(2A)-Ru(4A)	92.47 (5)	Pt(1A)-Ru(5A)-Ru(6A)	84.93 (6)
Ru(2A)-Pt(2A)-Ru(4A)	112.60 (6)	Pt(3A)-Ru(5A)-Ru(4A)	87.79 (6)
Ru(2A)-Pt(2A)-Ru(6A)	151.08 (6)	Pt(2A)-Ru(6A)-Ru(5A)	87.50 (6)
Ru(3A)-Pt(2A)-Ru(4A)	150.73 (6)	Pt(3A)-Ru(6A)-Ru(4A)	87.22 (6)
Ru(3A)-Pt(2A)-Ru(6A)	104.03 (6)	Ru(1A)-C(13A)-O(13A)	139 (2)
Pt(1A)-Pt(3A)-Ru(3A)	91.00 (5)	Ru(2A)-C(21A)-O(21A)	155 (2)
Pt(1A)-Pt(3A)-Ru(6A)	96.40 (5)	Ru(2A)-C(13A)-O(13A)	136 (2)
Pt(2A)-Pt(3A)-Ru(1A)	91.76 (5)	Ru(2A)-C(21A)-O(21A)	155 (2)
Pt(2A)-Pt(3A)-Ru(5A)	92.42 (5)	M-C(av)-O	176 (3)
Ru(1A)-Pt(3A)-Ru(5A)	112.33 (6)		

[a] Angles are in degrees. Estimated standard deviations in the least significant figure are given in parentheses.

Organometallics **1992,** *11,* 4009–4015 4009

Scheme I. In **3** the tenth metal atom remains attached to the complex by a hydride-bridged metal–metal bond and two μ_3-η^2 carbonyl ligands serving as four-electron donors. This μ_3-η^2 coordination type A is new although

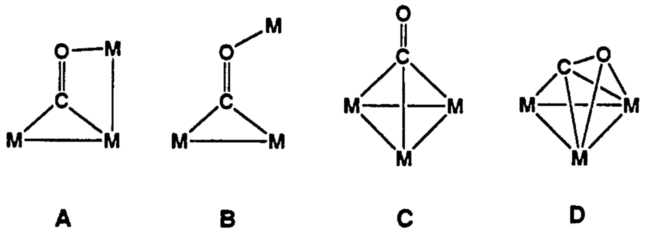

there are related examples of μ_3-η^2 carbonyl ligands where the oxygen-coordinated metal atom is not directly bonded to the other metal atoms, B.[21,22] Other examples of triply bridging carbonyl ligands include the μ_3-η^1 C,[22] a two-electron donor, and the μ_3-η^2 D, which serves as a six-electron donor.[23]

In the formation of **4** one metal atom was completely removed from the cluster. It seems likely that compound **3** could represent an intermediate species traversed in the course of the degradation of **2** to **4**. It is possible that the product obtained from the reaction of **1** with CO may eventually prove to be an analog of **4**.

Acknowledgment. These studies were supported by the National Science Foundation under Grant No. CHE-8919786. We wish to thank Dr. Istvan Horvath of Exxon Research and Engineering Co. for providing a sample of ^{13}CO for use in the labeling studies.

Supplementary Material Available: Tables of hydrogen atom parameters, anisotropic thermal parameters, and bond distances and angles for all four structural analyses (43 pages). Ordering information is given on any current masthead page.

OM920347D

---

[21] (a) Cotton, F. A.; Schwotzer, W. *J. Am. Chem. Soc.* **1983**, *105*, 4955. (b) Chisholm, M. H.; Hoffmann, D. M.; Huffman, J. C. *Organometallics* **1985**, *4*, 986.

[22] Horwitz, C. P.; Shriver, D. F. *Adv. Organomet. Chem.* **1984**, *23*, 219 and references therein.

[23] Herrmann, W. A.; Biersack, H.; Ziegler, M. L.; Weidenhammer, K.; Siegel, R.; Rehder, D. *J. Am. Chem. Soc.* **1981**, *103*, 1692.

Syntheses of $(\mu\text{-H})FeRu_2(\mu\text{-CX})(CO)_{10}$ (X = OMe, NMe_2) and $(\mu\text{-H})_3FeRu_2(\mu_3\text{-COMe})(CO)_9$. Ligand Substitution on $(\mu\text{-H})Fe_nRu_{3-n}(\mu\text{-CNMe}_2)(CO)_{10}$ (n = 1, 3)

Derrick S. Parfitt, Jeffrey D. Jordan, and Jerome B. Keister*

*Department of Chemistry, University at Buffalo, State University of New York,
Buffalo, New York 14214*

Received May 19, 1992

The new clusters $HFeRu_2(\mu\text{-CX})(CO)_{10}$ (X = OMe, NMe_2) have been prepared in low yield by metal fragment exchange. Hydrogenation of $HFeRu_2(\mu\text{-COMe})(CO)_{10}$ yields $H_3FeRu_2(\mu_3\text{-COMe})(CO)_9$. For X = NMe_2 reaction with PPh_3 gives $HFeRu_2(\mu\text{-CNMe}_2)(CO)_9(PPh_3)$ and $HFeRu_2(\mu\text{-CNMe}_2)(CO)_8(PPh_3)_2$ with all substitutions on Ru. Kinetic studies of substitution by PPh_3 on $HFe_3(\mu\text{-CNMe}_2)(CO)_{10}$ and on $HFeRu_2(\mu\text{-CNMe}_2)(CO)_{10}$ found that the mechanism involves rate-determining CO dissociation. The order of relative rates for substitution, $FeRu_2 > Fe_3 > Ru_3$, suggests that CO dissociation occurs from Fe. The higher rate for the mixed-metal cluster is attributed to labilization of the Fe center by the Ru "ligand".

The reactivities of mixed-metal clusters provide an opportunity to probe mechanisms.[1] We have used the relative reactivities of the clusters $HRu_{3-n}Os_n(\mu\text{-COMe})(CO)_{10}$ and $H_3Ru_{3-n}Os_n(\mu_3\text{-COMe})(CO)_9$ to determine the number of metal atoms which are involved in the transition state for reductive elimination of hydrogen from the latter clusters.[2] For both CO dissociation and H_2 elimination the relative rates are in the order $Ru_3 > Ru_2Os > RuOs_2 \gg Os_3$; the mixed-metal clusters are intermediate in reactivity between, but with rates closer to that of the most reactive of, the two homometallic analogs. However, the reactivities of mixed Ru/Fe trinuclear clusters have been shown to be different. For CO dissociation from $Fe_{3-n}Ru_n(CO)_{12}$ the mixed-metal clusters were the most reactive, the order of relative rates being Fe_2Ru (21) > $FeRu_2$ (12) > Fe_3 (4.6) > Ru_3 (1);[3] however, the site of substitution for the mixed Fe/Ru clusters is on Ru.[3,4] Complicating features are the lack of structural similarity throughout the series, with the number of bridging carbonyl ligands decreasing as the Ru content increases and only a small range in rate constants. Mixed Fe/Ru clusters have also been shown to be more active catalysts for the water gas shift reaction than the homometallic analogs.[5]

We report here the syntheses of the new mixed-metal alkylidyne clusters $HFeRu_2(\mu\text{-CX})(CO)_{10}$ (X = OMe, NMe_2) and their reactions with H_2 (X = OMe) and with

---

[1] (a) Gladfelter, W. L.; Geoffroy, G. L. *Adv. Organomet. Chem.* **1980**, *18*, 207. (b) Roberts, D. A.; Geoffroy, G. L. In *Comprehensive Organometallic Chemistry*; Wilkinson, G., Ed.; Pergamon Press: Oxford, U.K., 1982; Vol. 6, p 763.

[2] Keister, J. B.; Onyeso, C. C. O. *Organometallics* **1988**, *7*, 2364.

[3] (a) Shojaie, R.; Atwood, J. D. *Inorg. Chem.* **1987**, *26*, 2199. (b) Shojaie, A.; Atwood, J. D. *Organometallics* **1985**, *4*, 187.

[4] Venalainen, T., Pakkanen, T. *J. Organomet. Chem.* **1984**, *266*, 269.

[5] (a) Ford, P. C.; Rinker, R. G.; Ungermann, C.; Laine, R. M.; Landis, V.; Moya, S. A. *J. Am. Chem. Soc.* **1978**, *100*, 4595. (b) Ungermann, C.; Landis, V.; Moya, S. A.; Cohen, H.; Walker, H.; Pearson, R. G.; Rinker, R. G.; Ford, P. C. *Ibid.* **1979**, *101*, 5922.

0276-7333/92/2311-4009$03.00/0